Shock-cloud interactions in young gamma-ray supernova remnants: Evidence for cosmic-ray acceleration

NANTEN Submillimeter Observatory
NAGOYA UNIVERSITY
Career Development Project for Researchers of Allied Universities
INSTITUTE FOR ADVANCED RESEARCH NAGOYA UNIVERSITY

Hidetoshi Sano[1,2]* & Yasuo Fukui[1,2]

[1] Department of Physics, Nagoya University, Furo-cho, Chikusa-ku, Nagoya 464-8601, Japan (sano@a.phys.nagoya-u.ac.jp)
[2] Institute for Advanced Research, Nagoya University, Furo-cho, Chikusa-ku, Nagoya 464-8601, Japan

Abstract: In young supernova remnants (SNRs; ~2000 yrs old), interactions between the shockwave and interstellar neutral gas play a key element in understanding the origin of cosmic rays and their high-energy radiation. Fukui et al. (2012) demonstrated good spatial correspondence between the TeV gamma rays and total interstellar gas in the young SNR RX J1713.7–3946. This gives one of the essential conditions producing the hadronic gamma rays, and evidence for acceleration of cosmic ray protons up to 100 TeV. Subsequent studies showed similar results for young SNRs HESS J1731–347 (Fukuda et al. 2014), Vela Jr. (Fukui et al. 2017), and RCW 86 (Sano et al. 2019). For cosmic ray electrons, Sano et al. (2010, 2013, 2017a,b) revealed the synchrotron X-ray enhancement toward the dense molecular clouds in the SNRs RX J1713.7–3946, RCW 86, and superbubble 30 Doradus C. Owing to interactions between the shock and inhomogeneous gas distribution—dense gas ($\sim10^{3}$ cm^{-3}) clumps in low-density environments (~0.01 cm^{-3})—the magnetic field strength is significantly enhanced up to ~1 mG via the strong turbulent motion around the dense gas clumps. The X-ray hard spectra are reported toward the regions in which the shock-cloud interactions are strongly occurred, indicating that cosmic rays are efficiently accelerated to the higher maximum energy (Sano et al. 2015; Babazaki et al. 2018). In this poster, we introduce our recent studies of shock-cloud interactions toward the young SNRs bright in both the TeV gamma rays and synchrotron X-rays.

Topic 1: Origin of Cosmic-Ray Protons

1. Cosmic-rays & Supernova Remnants

☑ It is a longstanding question how cosmic-ray (CR) protons are accelerated in interstellar space.

☑ Supernova remnants (SNRs) are the most likely candidates for acceleration because the high-speed shock waves offer an ideal site for the DSA [e.g.,1,2].

2. Hadronic gamma-rays from young SNRs

☑ TeV gamma-rays from young SNRs are mainly produced by relativistic CR protons and/or electrons close to PeV through two mechanisms, called hadronic or leptonic processes (Fig.1).

☑ Numerous attempts have been made to distinguish the two processes using broadband spectral modeling [e.g.,3]. In most cases, however, it is difficult to distinguish between hadronic and leptonic gamma-rays by the spectral modeling alone (Fig 1., [e.g., 3,4,5]).

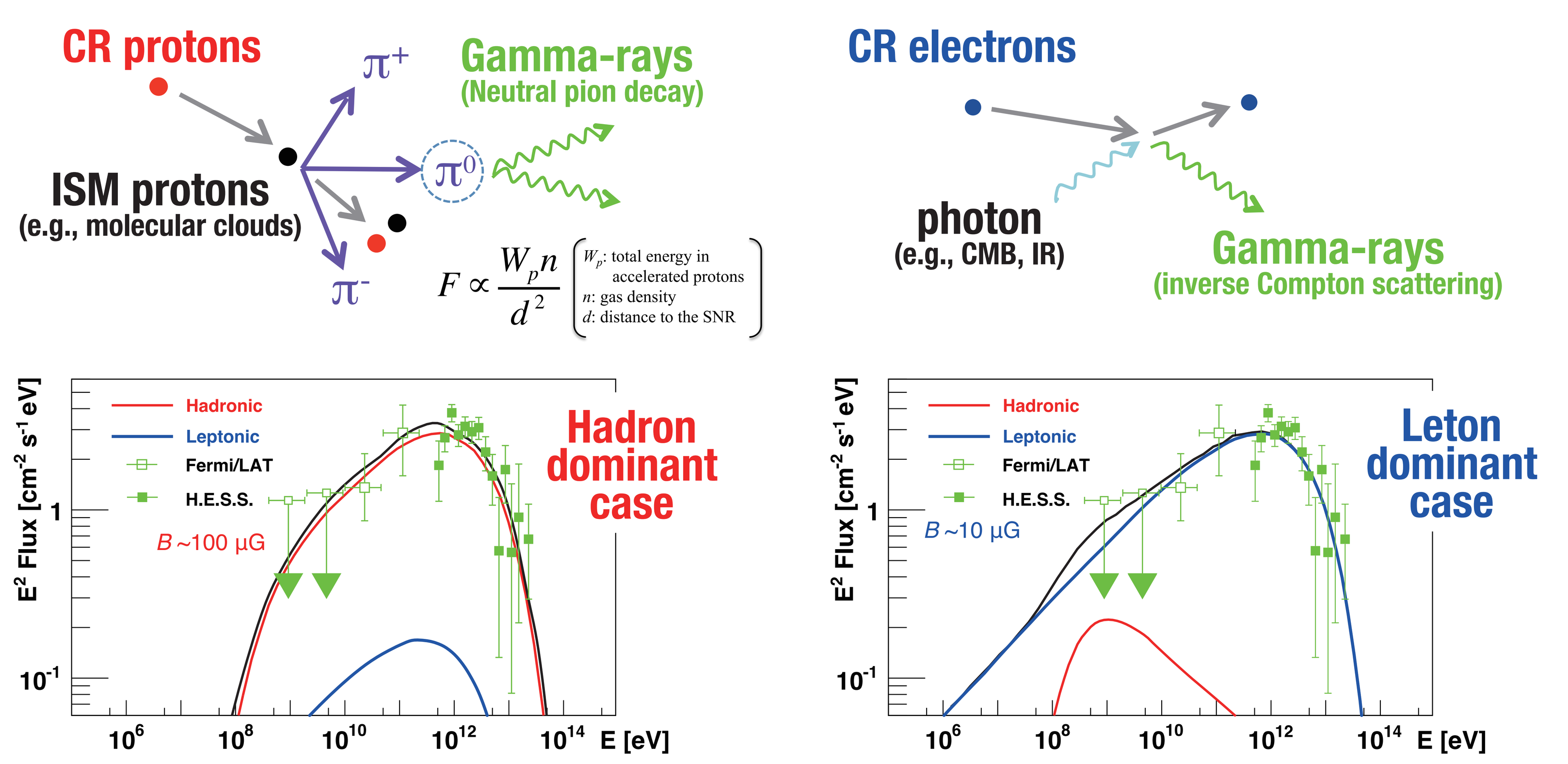

Fig. 1: (upper panels) Schematic images of hadronic and leptonic gamma-rays. (lower panels) Results of spectral modeling toward TeV gamma-ray SNR RCW 86 [3].

3. Spatial corespondence between the ISM protons & gamma-rays

☑ The hadronic gamma-ray flux is proportional to the target-gas density.

☑ We presented good spatial correspondence between TeV gamma-rays and ISM protons in the young SNRs RX J1713.7–3946, Vela Jr., HESS J1731-347, and RCW 86. This provides one of the essential conditions for gamma-rays to be predominantly of hadronic origin (Fig. 2, [6-9]).

☑ The total energy of CR protons, $\sim10^{48}$–10^{49} erg, derived using ISM density gives a lower limit.

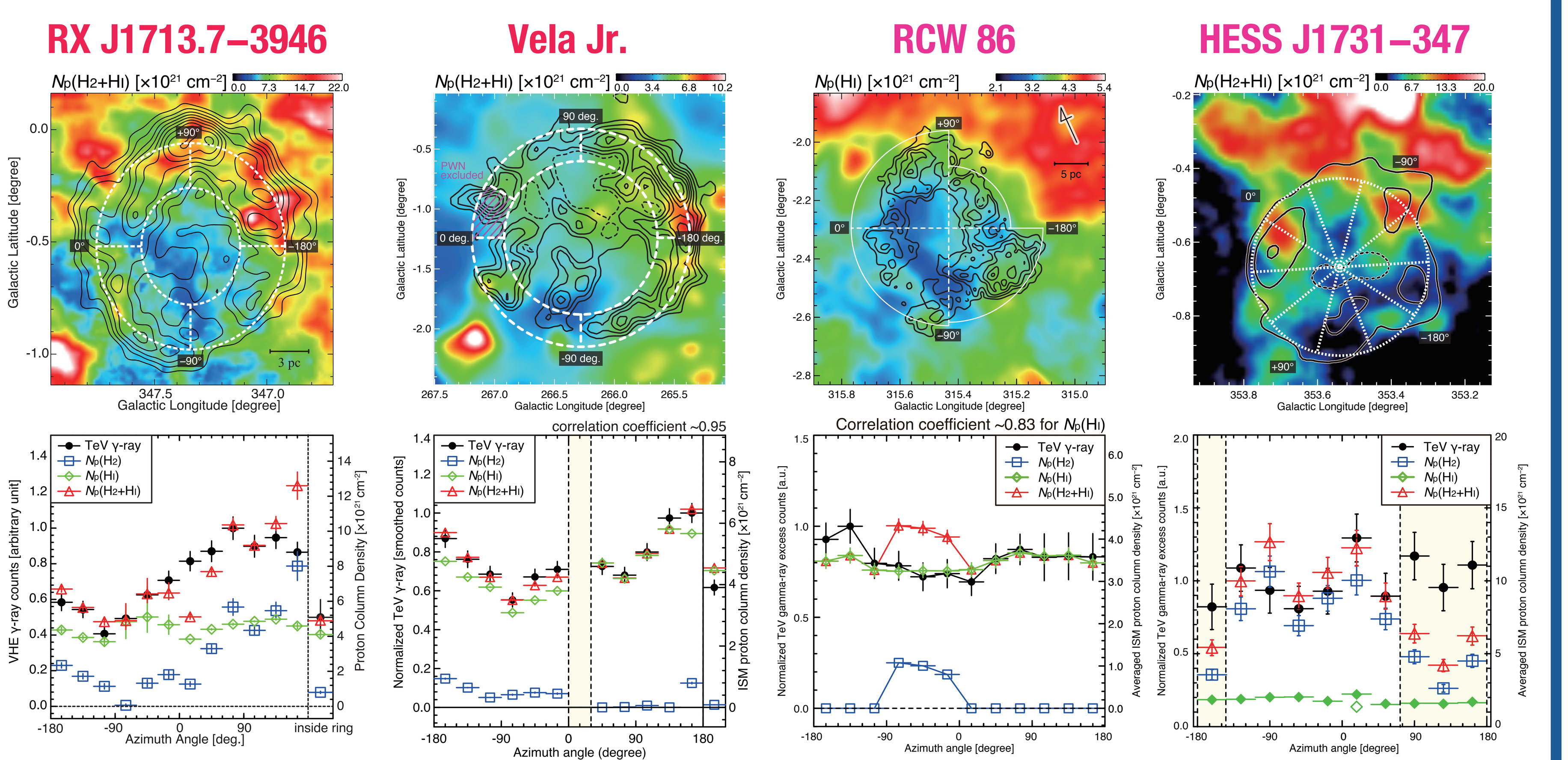

Fig. 2: (upper panels) ISM proton column density maps superposed on the TeV gamma-ray contours toward RX J1713.7−3946 [6], Vela Jr. [7], RCW 86 [8], and HESS J1731−347 [9]. The ISM proton column density was derived by using both the CO and HI line emission. (lower panels) Azimuthal profiles of normalized TeV gamma-ray, $Np(H_2)$, Np(HI), and $Np(H_2 + HI)$, which are averaged every 30° in the azimuthal angle within the region indicated by the white solid line in each upper panel.

4. Future prospects: Leading the ISM–gamma-ray science using CTA

☑ Cherenkov Telescope Array (CTA) will provide us with high angular resolution (up to ~30") and high sensitivity (10 times deeper than the previous results) → increasing number of targets

☑ We have confirmed the CTA performance by using the Monte Carlo simulation [10].

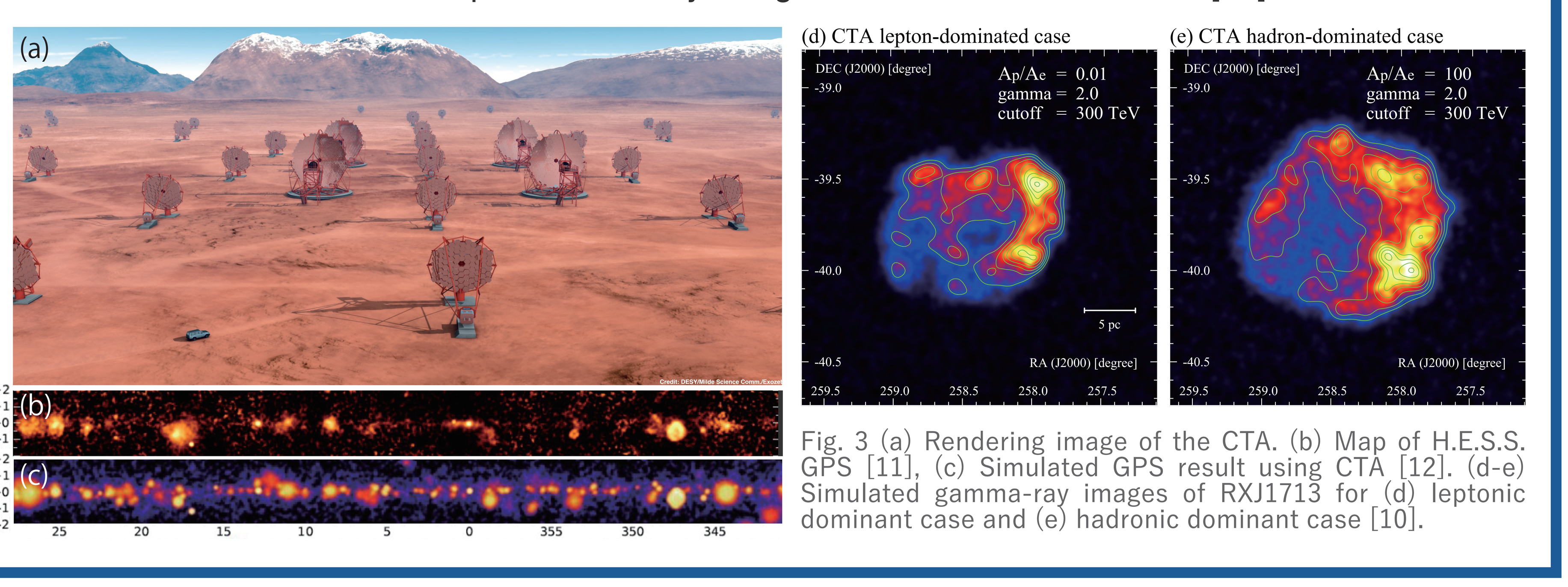

Fig. 3 (a) Rendering image of the CTA. (b) Map of H.E.S.S. GPS [11]. (c) Simulated GPS result using CTA [12]. (d-e) Simulated gamma-ray images of RXJ1713 for (d) leptonic dominant case and (e) hadronic dominant case [10].

Topic 2: Efficient Acceleration of CR Electrons via Shock-Cloud Interactions

1. Classical DSA model

☑ CRs cannot be accelerated to PeV via the classical DSA model [e.g., 1,2].

☑ Classical DSA model assumes uniform ISM, but the actual ISM shows highly inhomogeneous.

2. X-ray enhancement toward the shocked gas clumps

☑ Sano et al. found synchrotron X-ray enhancement around the shocked gas clump in the SNRs RX J1713.7–3946, RCW 86, and superbubble 30 Doradus C [13,14,15,16].

☑ The photon index of synchrotron X-rays also show small values (< 2.4) toward the shocked gas clumps in RX J1713.7-3946 and 30 Doradus C [17,18].

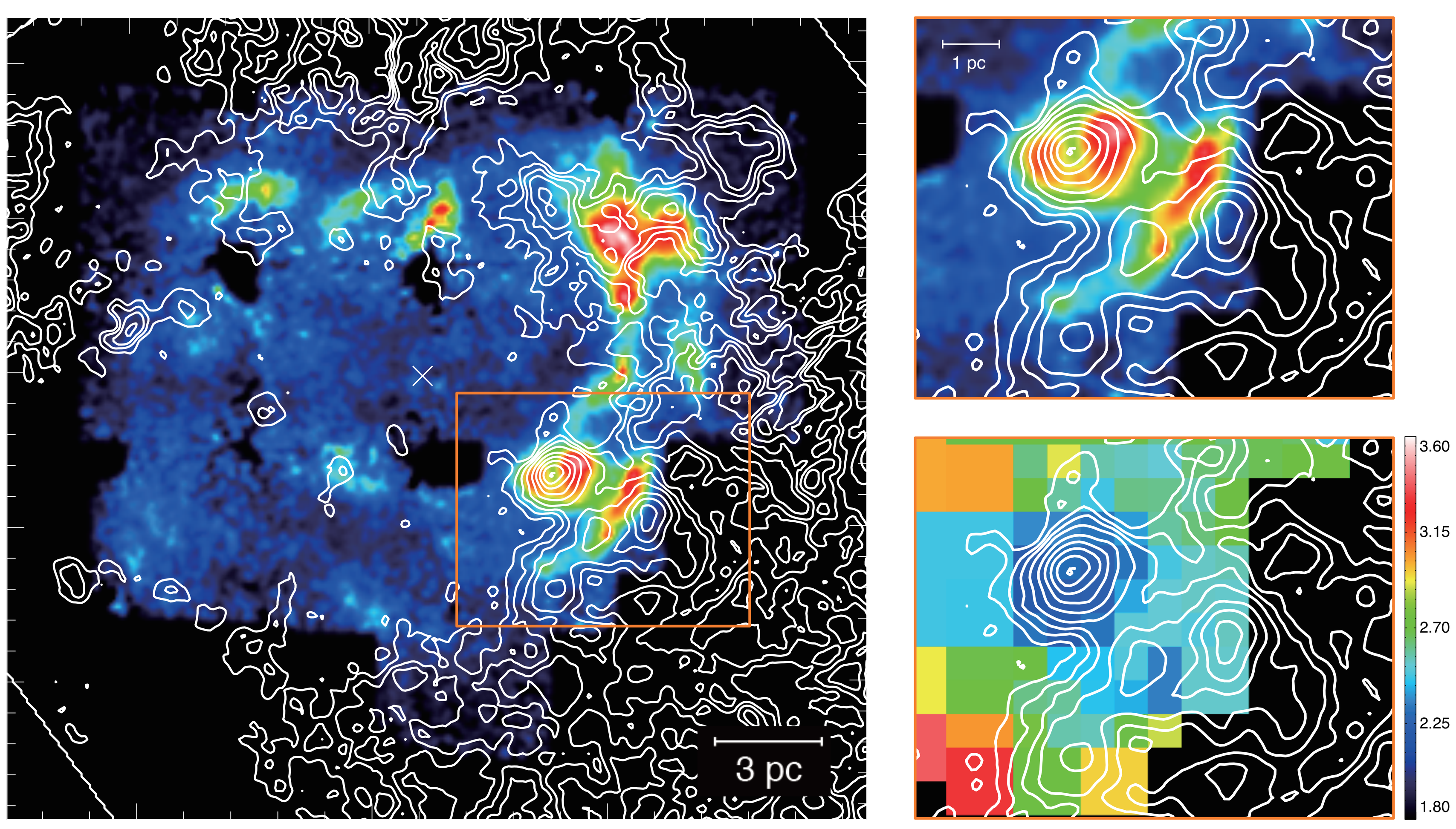

Fig. 4: (left panel) *Suzaku* synchrotron X-rays (E: 5−10 keV) overlaid with the NANTEN2 $^{12}CO(J=2-1)$ integrated intensity contours [14]. (top right panel) Enlarged view of CO clump C. the dense gas cores are rim-brightened in synchrotron X-rays in sub-pc scale. (bottom right panel) Photon index map of synchrotron X-rays overlaid with the CO contours [17].

3. Shock propagation into the inhomogeneous medium

☑ The ambient HI gas was completely evacuated by strong stellar winds from the massive progenitor, but dense molecular clouds can survive in the wind because of their high-density.

☑ The forward shock propagates through the wind-bubble with no CR electrons also, while the shock waves toward the clouds are stalled, while the shock waves toward the clouds are stalled.

☑ Shock–cloud interactions induce shock deformations and turbulence. The turbulent dynamo effect amplifies the magnetic field up to ~1 mG that enhances synchrotron emission.

☑ CR electrons are possibly re-accelerated via turbulence, reflected shocks, and/or magnetic reconnection in the downstream. We therefore observe the small photon index in the downstream.

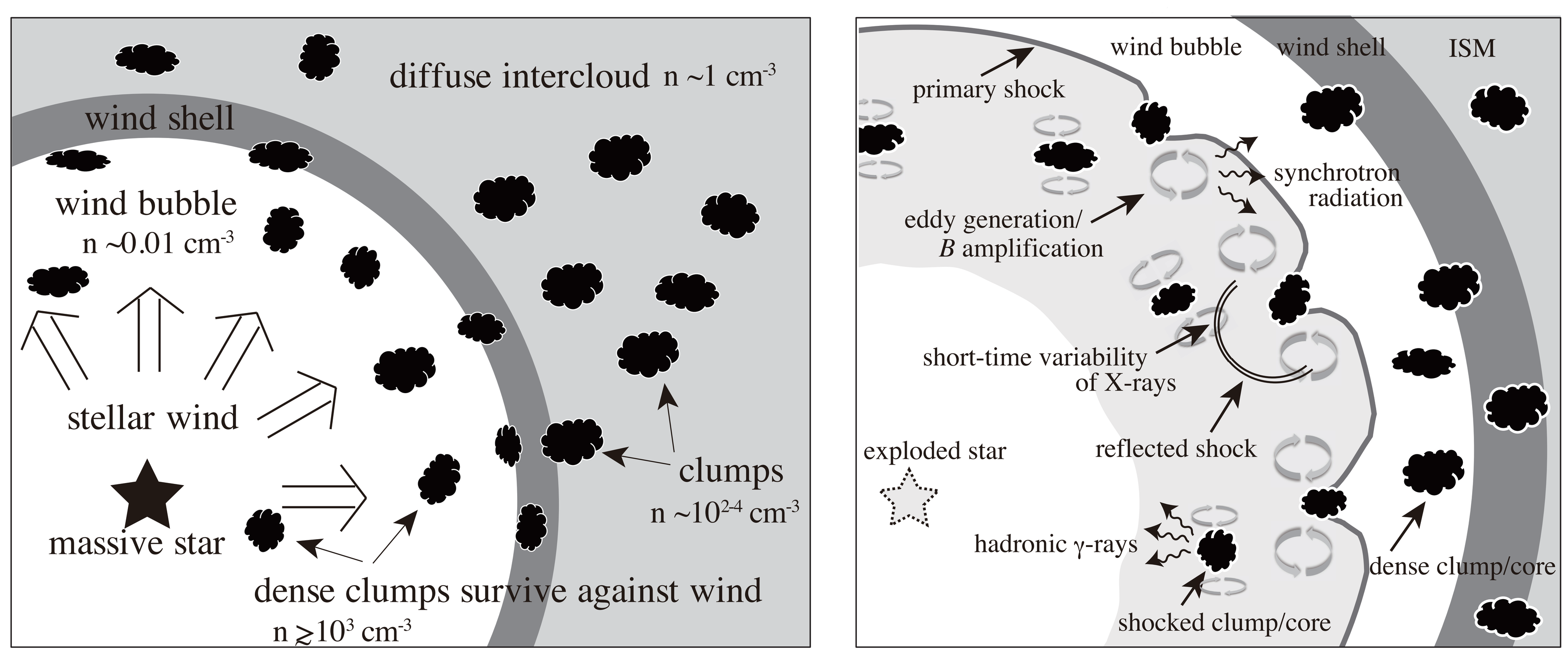

Fig. 4: (left panel) Schematic view of wind bubble expanding in a cloudy ISM [5]. Diffuse intercloud gas is swept by the stellar wind, while dense cloud cores and clumps can survive in the wind. Density in the wind bubble is much smaller than the intercloud gas density that is determined by the evaporation of the wind shell by thermal conduction. (right panel) Schematic picture of the shock–cloud interaction model [5]. The primary forward shock wave propagates through the cloudy wind bubble, where particle acceleration operates. Transmitted shock waves in the clouds are stalled, which suppresses thermal X-ray line emission and particle acceleration in the clouds. Shock–cloud interactions induce shock deformations and turbulent eddies. The turbulent dynamo effect amplifies the magnetic field that enhances synchrotron emission. Secondary reflected shock waves are generated when the primary shock hits clouds that induce the short-time variability of synchrotron X-rays where magnetic field strength is ~1 mG around shocked clouds. Hadronic gamma rays are emitted from dense clouds illuminated by accelerated protons whose photon index can be p − 1/2 = 1.5 for p = 2.

References

[1] Bell 1978, MNRAS, 182, 147, [2] Blandford & Ostriker (1978), ApJL, 221, 29, [3] HESS Col. et al. (2018), A&A, 612, 4, [4] Inoue et al. (2009), ApJ, 695, 825, [5] Inoue et al. (2012), ApJ, 744, 71, [6] Fukui et al. (2012), ApJ, 746, 82, [7] Fukui et al. (2017), ApJ, 850, 71, [8] Sano et al. (2019), ApJ, 876, 37, [9] Fukuda et al. (2014), ApJ, 788, 94, [10] Acero et al. (2017), ApJ, 840, 74 (corresponding author), [11] H.E.S.S. Col. et al. (2018), A6A, 612, 61, [12] CTA Consortium (2019), Science with the Cherenkov Telescope Array, [13] Sano et al. (2010), ApJ, 724, 59, [14] Sano et al. (2013), ApJ, 778, 59, [15] Sano et al. (2017a), JHEAp, 15,1, [16] Sano et al. (2017b), ApJ, 843, 61, [17] Sano et al. (2015), ApJ, 799, 175, [18] Babazaki et al. (2018), ApJ, 864, 12